Molecular Neurobiology (2019) 56:6371–6385
https://doi.org/10.1007/s12035-019-1527-0

Delayed Galectin-3-Mediated Reprogramming of Microglia After Stroke is Protective

Reza Rahimian[1,4] · Starlee Lively[2] · Essam Abdelhamid[1,4] · Melanie Lalancette-Hebert[1,4] · Lyanne Schlichter[2] · Sachiko Sato[3] · Jasna Kriz[1,4]

Received: 11 December 2018 / Accepted: 13 February 2019 / Published online: 23 February 2019

Abstract

Galectin-3 (Gal-3), a β-galactoside-binding lectin, has recently emerged as a molecule with immunoregulatory functions. We investigated the effects of Gal-3 on microglia morphology, migration, and secretory profile under physiological conditions and in the context of ischemic injury. We show that in the control conditions, exposure to recombinant Gal-3 increases microglial ramification and motility in vitro and in vivo via an IL-4-dependent mechanism. Importantly, after stroke, Gal-3 exerted marked immune-modulatory properties. Delivery of Gal-3 at 24 h after middle cerebral artery occlusion (MCAO) was associated with an increase in Ym1-positive microglia and decrease in iNOS. Analysis of cytokine profiles at the protein level revealed downregulation of pro-inflammatory cytokines and a marked upregulation of the anti-inflammatory cytokine, IL-4, 24 h after i.c.v. injection of Gal-3. Importantly, the observed shift in cytokines in microglia was associated with a significant decrease in the infarct size. Taken together, our results suggest that when delivered well after ischemic injury, Gal-3 might fine tune innate immunity and induce a therapeutic shift in microglia polarization.

Keywords Galectin-3 · Microglia · Interleukin 4 · Stroke · Innate immunity

Introduction

Microglia are self-renewing and long-lived resident macrophage-like cells of the brain. The current view is that, once activated, microglial cells acquire a wide variety of polarization phenotypes ranging from highly pro-inflammatory and toxic to alternative activated "healing cells" that contribute to recovery after brain damage [1, 2]. Indeed, activated microglial cells may contribute to post-ischemic inflammation by producing tumor necrosis factor-alpha (TNF-α), interleukin(IL)-1 beta (IL-1β), reactive oxygen species, and other neurotoxic, pro-inflammatory molecules [3, 4]. However, they also contribute to resolution of inflammation and tissue repair by producing IL-4, IL-10, and transforming growth factor beta (TGF-β) [4, 5]. For instance, many groups, including ours, have demonstrated a neuroprotective role for microglial cells by their capacity to produce homeostatic cytokines [6] and growth factors [7–10] or by playing a role in protective phagocytosis [11]. Considering the complex role of microglia in the brain's response to injuries and neurodegeneration, anti-inflammatory strategies should not merely focus on general suppression of inflammatory responses, but rather on favoring the beneficial over detrimental actions of microglia [12]. Over the past years, we investigated several molecular pathways involved in the post-ischemic inflammatory cascade and have identified galectin-3 (Gal-3) as a key player in the ischemic injury-induced microglial activation and proliferation [10, 13].

Gal-3, one of a 15-member family of galectins, is a β-galactosidase-binding lectin [14, 15]. Mounting evidence suggests that galectins, including Gal-3, act as endogenous

Electronic supplementary material The online version of this article (https://doi.org/10.1007/s12035-019-1527-0) contains supplementary material, which is available to authorized users.

✉ Jasna Kriz
jasna.kriz@fmed.ulaval.ca

[1] CERVO Brain Research Centre, Université Laval, Québec, QC G1J 2G3, Canada

[2] Krembil Research Institute, University Health Network, Toronto, ON, Canada

[3] Glycobiology Laboratory, Research Centre for Infectious Disease, Université Laval, Quebec, QC G1V 4G2, Canada

[4] Department of Psychiatry and Neuroscience, Faculty of Medicine, Université Laval, 2601 Chemin de la Canardiere, Québec, QC G1J 2G3, Canada

modulators of the inflammatory response in the periphery; however, their roles in the brain are less defined [15–18]. Our previous work revealed that Gal-3 is expressed in insulin-like growth factor 1 (IGF-1) labeled, proliferating microglia as early as 48 h after stroke, and that sustained Gal-3 deficiency exacerbates ischemic injury [10, 13]. On the other hand, in a model of global ischemia, Gal-3-dependent-Toll-like receptor 4 (TLR4) activation was associated with increased neuron damage in the hippocampus 24 h after initial injury [19]. These findings underline the complex and potentially time-dependent role of Gal-3 in the modulation of the microglia functional profile [20].

Evidence suggests that inhibition of TLR signaling, especially TLR2, within the initial 24 h after ischemic injury is protective [21, 22]. Conversely, disrupting TLR2 signaling after this acute period has been associated with a delayed increase in the ischemic lesion [22]. Importantly, Gal-3 might form complexes with TLRs (TLR2 and TLR4) and with different trophic factor receptors, including IGF-1 [13, 23]. Because protective microglial phenotypes, characterized by secretion of trophic factors, occur more than 24 h post-injury, we hypothesized that the timing of delivery after post-ischemic injury would determine the functional impact of Gal-3. To test our hypothesis, we initiated Gal-3 treatment 24 h after stroke. Here, we show that a single intracerebroventricular (i.c.v.) injection of recombinant Gal-3 at 24 h after stroke shifts microglia polarization toward alternative activation, diminishes pro-inflammatory cytokine levels, and confers neuroprotection. Under physiological conditions and in the primary microglia cultures, Gal-3 induces an IL-4-mediated morphological transformation of microglia into a more ramified state. Alongside the morphological modulation, Gal-3 drives the cytokine profile of microglia toward anti-inflammatory phenotypes and induces microglia migration. A better understanding of the functions of Gal-3 and its downstream signaling pathways in microglia will open new avenues for innovative drug discovery for stroke.

Materials and Methods

Experimental Animals

All experiments are performed on Toll-like receptor 2 (TLR2)-fluc-GFP transgenic mice and WT littermates (C57BL/6 background), in which luciferase and GFP reporters are driven under the transcriptional control of the murine TLR2 gene promoter. The TLR2-Fluc-GFP transgenic mice were detected by the amplification of the luciferase transgene as described previously [24]. All experimental procedures were approved (protocol no. 017-133) by the Laval University Animal Care Ethics Committee and are in accordance with the Canadian Council on Animal Care.

Surgical Procedures and Treatment

MCAO and Stroke Area Evaluation

Unilateral transient focal cerebral ischemia was induced by middle cerebral artery occlusion (MCAO) for 1 h followed by 48 h to 4 days reperfusion time. The MCAO was performed on 2–3-month-old male mice (20–25 g). The surgery was done as previously described [13, 22]. Briefly, the animals were anesthetized with 2% isoflurane in 100% oxygen at a flow rate of 1.8 L/min. To avoid cooling, the body temperature was monitored and maintained at 37 °C with a heating pad. The internal carotid artery (ICA) was isolated and carefully separated from the adjacent tissue and a 12-mm-long 6–0 silicon-coated monofilament suture was inserted via the proximal external carotid artery (ECA) into the ICA and then into the circle of Willis to occlude the MCA. The area of infarction was quantified with ImageJ (version 1.42q for Windows, National Institutes of Health), and infarct area was calculated as percentage of control, non-stroke area in the contralateral hemisphere with appropriate corrections for brain edema. As previously described, the analyses were performed on the cresyl-violet-stained sections [22, 25].

Injections of the Recombinant Gal-3

Experimental animals were anesthetized and placed onto the stereotaxic apparatus (David Kopf Instruments). The recombinant Gal-3 was delivered in two distinct experimental conditions: Control, non-ischemic brain: Gal-3 or Mock (100 ng/2 μl) was injected to WT mice via intracortical (IC) route (injection site coordinates: L − 2 mm, AP − 2 mm, DV − 1.25 mm), and after 24 h, the brains were collected for morphology studies.

After stroke: At 24 h following MCAO, experimental animals received a single i.c.v. injection (L − 1.5 mm, AP − 1 mm, DV − 2 mm) of Gal-3 (100 ng/mouse) or Mock. Both Gal-3 and mock were dissolved in sterile phosphate-buffered saline (PBS), and volume of injection was 2 μl for each mouse. TLR2-fluc-GFP was euthanized at different reperfusion time for biochemical, immunofluorescence, and stroke volume studies.

Administration of Glucosamine

Glucosamine treatment (150 mg/kg/day, i.p. in saline 0.9%) was started 2 h after stroke and continued for three subsequent days. Three days after, MCAO mice were euthanized for biochemical and immunofluorescence experiments.

Recombinant Gal-3

Recombinant Gal-3 was purified by affinity chromatography using lactosyl-sepharose (MilliporeSigma, Burlington, MA,

USA) from an extract of *Escherichia coli* overexpressing Gal-3, as previously described [26]. Bound Gal-3 was released with PBS containing 150 mM lactose. A HiPrep 26/10 Desalting Column (GE Healthcare Life Sciences, Little Chalfont St. Giles, UK) was then used to remove the lactose from the Gal-3 fraction. Next, the Gal-3-enriched eluate was passed through an ActiClean Etox column (Sterogene Bioseparations, Carlsbad, CA, USA) to ensure that the endotoxin level was less than 1 pg/mg. Mock control solution was prepared following the same purification procedure using the extract of *E. coli*, which does not express Gal-3. The specific (oligosaccharide-binding) activity of Gal-3 was tested before each experiment by using it to induce hemagglutination [27–29].

Tissue Collection and Immunofluorescence Analysis

Animals were anesthetized via an intraperitoneal (i.p.) injection of ketamine/xylazine (100–10 mg/kg) and transcardially perfused with PBS, followed by PBS-buffered 4% paraformaldehyde (PFA) at pH 7.4. Tissue samples were then fixed for 2 days in 4% PFA and equilibrated in phosphate-buffered 20% sucrose for 48 h. Brains were embedded in Tissue-Tek (O.C.T. compound; Sakura), frozen at − 80 °C overnight, and cut into coronal sections (35 μm thick) with a cryostat and stored at − 20°C [26]. The brain sections were then incubated overnight at room temperature using primary antibodies, 1:500 rabbit polyclonal anti-Iba1 (Wako), 1:500 rat anti-Gal-3 (ATCC), 1:500 rabbit polyclonal anti-Ym1 (Stem Cell Technologies), 1:500 rabbit polyclonal anti-Arginase1 (Santa Cruz), 1:1000 rabbit polyclonal anti-Ki-67 (Millipore), and 1:50 mouse monoclonal anti-IGF-1 (Millipore). After washing in TBS, the sections were incubated in corresponding fluorescent goat secondary antiserum (Invitrogen) [26]. Alexa Fluor® 488 phalloidin (Thermo Fisher Scientific) was used to study microglia morphology following Gal-3 treatment. All pictures have been taken using a Leica CTR 500 epifluorescence microscope.

Histological Evaluation of the Size of Infarction

The size of infarction was evaluated at 4 days after MCAO in Gal-3-treated animals. The samples were fixed overnight in 4% PFA and equilibrated in phosphate-buffered 20% sucrose for 48 h. Brains were embedded in Tissue-Tek (O.C.T. compound) and cut into coronal sections with a cryostat. Tissue sections (all the stroke area region $n = 6$/group) were stained with cresyl-violet and were digitized with a Leica DM 5000B. The area of infarction, direct stroke area, was quantified with ImageJ (version 1.42q, NIH), and infarct area was calculated as a percentage of control, non-stroke area in the contralateral hemisphere with appropriate corrections for brain edema [25]. Note that in Fig. 4k–l, the area around the cresyl-violet stained brains was removed in Adobe Photoshop.

In Vivo Bioluminescence Imaging

As previously described [13, 24, 30], the images were obtained using IVIS® 200 Imaging System (Perkin Elmer); 25 min before imaging, mice received an i.p. injection of D-luciferine (150 mg/kg; Perkin Elmer). Region of interest measurements on the images were used to convert surface radiance (photons/s/cm^2/sr) to source flux or total flux of photons expressed in photons/s (p/s). The data are represented as pseudo-color images indicating light intensity (red and yellow, most intense), superimposed over grayscale reference photographs [31].

Cytokine Arrays

Cytokine arrays were carried out using a mouse antibody array (Raybio®Mouse Inflammation Antibody Array 1.1, Ray Biotech, #AAM-INF-1L) as described [22]. Protein lysate was obtained by homogenization of mouse brains in 1× Cell Lysis Buffer (included in the Ray Biotech kit) supplemented with Protease inhibitor cocktail (Sigma #P8340). Samples for each group (3 mice/group) were pooled and incubated with the array membrane overnight at 4 °C. The membranes were then processed according to the Raybiotech protocol. Membranes were exposed to X-ray film (Kodak film Biomax MR1, #8701302) and analyzed using ImageJ as described [10, 13, 22].

Western Blotting

Total protein extracts were obtained from the ipsilateral hemisphere of the brain 48 h after cerebral ischemia by homogenization in a 1× Cell Lysis Buffer (included in the Ray Biotech kit) with Protease inhibitor cocktail (Sigma #P8340). The protein lysates from different samples were quantified by Bradford assay (detection at 595 nm). Samples containing 20 μg of protein were boiled in SDS-mercaptoethanol sample buffer, separated on 10% sodium dodecyl sulfate-polyacrylamide gel electrophoresis (SDS-PAGE) and electrically transferred to nitrocellulose membranes. Non-specific binding was blocked by preincubation of the nitrocellulose membrane in PBS containing 0.1% Tween 20 (PBS-T) and 5% skimmed milk for 1 h. The nitrocellulose was then incubated overnight at 4 °C with antibodies against the targeted proteins as follows: 1:500 anti-iNOS (BD Biosciences), 1:500 rabbit anti-Mgat5 (Abcam), 1:500 rabbit polyclonal anti-Ym1 (Stem Cell Technologies), 1:500 rabbit polyclonal anti-IL-4 receptor alpha (Santa Cruz), 1:1000 rabbit polyclonal anti-Iba-1 (Wako), 1:500 rabbit anti-Gal-3 (Cell signaling), 1:250 rabbit anti-Arginase-1 (Santa Cruz), 1:250 rabbit anti-TNF-α (Abcam), 1:250 rabbit anti-CCL5 (Abcam), and 1:20000

mouse anti-actin (Millipore) [25]. Primary antibody was detected with HRP-conjugated anti-rabbit or anti-mouse antibody (1:2000–1:5000), and blots were developed using an enhanced chemiluminescence detection system (ECL kit; Thermo Fisher Scientific). The density of the specific bands was quantified with ImageJ software and normalized to β-actin as a housekeeping protein.

Immunoprecipitation

Immunoprecipitation experiments were performed using the Dynabeads standard protocol from Invitrogen. Gal-3 antibody was first preincubated for 1 h with Dynabeads coupled with protein G. Then, 300 μg of proteins from each microglial cell culture (treated or non-treated with Gal-3) was incubated overnight with the Dynabeads at 4 °C. After several washes, 2× Laemmli buffer was added to the beads and incubated at 95 °C for 10 min. The eluate was collected using the magnetic device. As previously described, the eluate was run on a SDS-PAGE gel followed by a regular Western blotting using the IL-4 receptor alpha antibody (Santa Cruz) [22]. Same experiment was repeated for precipitation of IL-4 receptor alpha with its specific antibody, and the membranes were stained with anti-Gal-3 antibody (Cell signaling) to detect co-immunoprecipitated Gal-3.

Primary Cell Culture

As previously described, the primary cell cultures were derived from the brains of the adult, 8–9-week-old C57BL/6 wild-type mice. The mice were anesthetized by isoflurane 3% and transcardially perfused with ice-cold saline (Hospira) supplemented with 2 units/ml heparine (Sigma-Aldrich). The whole brain was extracted and placed in ice-cold Hibernate medium [Hibernate A medium (BrainBits LLC) supplemented with B-27 (1×) and 0.5 mM GLUTAMAX-I, L-alanyl-L-glutamine (Gibco, Invitrogen)] [13]. After mechanical dissociation, 5–6 brains were incubated in a 0.25% Trypsin-EDTA solution (Sigma) containing 250K U/ml of DNase I (Sigma). Following centrifugation, the pellet was resuspended in 2 ml of 37% Percoll that was overlaid 2 ml of 70% Percoll in a 5-ml centrifuge tube and centrifuged at 600×*g* for 40 min at room temperature with slow acceleration and no stop-brake. Cells were collected from the interphase, washed with dPBS and kept in culture medium. Cells were plated on culture-treated glass slides (Becton Dickinson) as 1,250,000 cells/ml and incubated at 37 °C in 95% air/5% CO_2 humidified culture incubator. At 4 days in vitro (DIV), cells were treated with glutamate (100 μM) for 15 min followed by 24-h incubation with Gal-3 (5 μM). For morphological studies, microglia were treated with Gal-3 (5 μM) in the presence or absence of IL-4 receptor blocker (CD124; 50 μg/ml).

Migration Assay

Microglia were seeded at 30,000 cells on the inner well of 8-μm Transwell™ inserts (VWR, Mississauga, ON) and allowed to settle for 30 min at 37°C and 5% CO2 before adding MEM with 2% FBS to the upper and lower wells. After 30 min, cells were treated with PBS with 0.1% BSA (control) or recombinant mouse Gal-3 (0.1, 1 or 5 μg/ml; R&D Systems Inc.) and cultured for 24 h. Microglia were then fixed in 4% PFA for 10 min at room temperature and rinsed with PBS. The inner well was swirled with a Q-tip to remove stationary cells. Cells that had migrated to the underside of the filter were stained with 0.3% crystal violet for 1 min, and rinsed in water to remove unbound dye. Migrated cells were counted (5 random fields/filter) at 20× magnification using an Olympus CK2 inverted microscope (Olympus, Tokyo, Japan). For each culture, cell counts obtained from Gal-3-treated cells were normalized to the control. Data are presented as mean ± SEM, and analyzed with a 1-way analysis of variance (ANOVA) followed by Tukey's post-hoc test using GraphPad Prism ver 5.01 (GraphPad Software, San Diego, CA). [32].

Real-Time Polymerase Chain Reaction

Real-time quantitative RT-PCR (qRT-PCR) analysis was carried out as the most sensitive method applied so far for quantification of differences in mRNAs. The main feature of this technique is use of a fluorescent dye, here SYBR Green, which emits fluorescence upon binding the double-stranded DNA. Therefore, the amount of fluorescence detected during the extension phase is proportional to the number of amplicons. In order to amplify cDNA, the polymerase chain reaction was performed using a StepOnePlus real-time PCR System (Applied Biosystems, CA, USA) with β-actin as the internal standard. Total volume of the reaction was 12.5 μl which contained 10 pmol of each primer, 6 μl of Power SYBR Green PCR Master Mix 2×, and 1.2 μl of template. The holding stage (95 °C for 5 min) was followed by the cycling stage (denaturation 10 s at 95 °C, combined annealing/extension 30 s at 60 °C), and the number of cycles was 40 [33]. HPRT1 was used as housekeeping gene in this study. The sequences of forward and reverse primers are listed in Table 1.

Statistical Analysis

Student's *t* test was employed to compare Gal-3-treated and non-treated groups following MCAO. When more than two groups were compared, one-way ANOVA was used. Tukey's post hoc was employed for multiple comparisons. In the scratch wound migration assay, Dunnett's post hoc test was used. All groups passed the normality test. For large sample sizes (imaging and stroke volume assays) D'Agostino–Pearson test was used to test normal distribution, while for smaller sample sizes, Shapiro–Wilk was employed. Statistical analyses were performed using the GraphPad Prism 6 software (GraphPad, La Jolla, CA).

Table 1 Primers used for real-time qPCR

Gene	Forward primer (5′–3′)	Reverse primer (5′–3′)
IL-6	GTCCTTCCTACCCCAATTTCCAA	GAATGTCCACAAACTGATATGCTTAGG
TNF-α	CCAGACCCTCACACTCAGATCATC	CCTTGAAGAGAACCTGGGAGTAGAC
IL-β	TCAAATCTCGCAGCAGCACATC	CCAGCAGGTTATCATCATCATCCC
IGF-1	GCCCCACTGAAGCCTACAAAAG	GCAGCTTCGTTTTCTTGTTTGTCG
IL-4	TTGTCATCCTGCTCTTCTTTCTCG	TCCCTTCTCCTGTGACCTCGTT
TGF-β1	ATGGAGCTGGTGAAACGGAAG	GTTGTTGCGGTCCACCATTAG
HPRT1	CAGGACTGAAAGACTTGCTCGAGAT	CAGCAGGTCAGCAAAGAACTTATAGC

Results

Gal-3 Alters Microglia Secretory Profile, Morphology, and Migration Patterns In Vitro

We previously demonstrated that targeted disruption of the Gal-3 gene significantly alters microglia activation and decreases microglia proliferation [13]. Defective microglia activation/proliferation was further associated with a significant increase in the size of the ischemic lesion, increase in the number of apoptotic neurons, and a marked deregulation of IGF-1 levels [13]. Importantly, in vitro analysis of Gal-3 KO microglia in the context of glutamate-induced excitotoxic injury showed an inability of these cells to adequately upregulate the innate immune response and expression of phagocytic markers, such as CD68 [13]. Because Gal-3 deficiency was associated with a marked deregulation in microglia activation patterns, here we asked to what extent the addition of recombinant Gal-3 would affect and/or restore activation profiles of microglial cells. First, we analyzed the effects of Gal-3 on microglia polarization and secretory profile. As previously described, we used a low-dose glutamate treatment to induce in vitro excitoxicity in primary microglia cell cultures [13]. The microglia cytokine profile was evaluated using RT-PCR analysis of selected cytokines and growth factors in baseline conditions and following Gal-3 and glutamate treatments. As expected, in vitro glutamate treatment increased expression of the pro-inflammatory cytokines, IL-1β and TNF-α, in primary microglial cell cultures (Fig. 1a–f), while addition of exogenous Gal-3 reduced the glutamate-induced increase of inflammatory molecules to control-baseline values (Fig. 1b, c). Conversely Gal-3 treatment increased levels of IL-6 and IL-4, and the growth factors, IGF-1 and TGF-β (Fig. 1a, d–f) (***$P < 0.001$; **$P < 0.01$; *$P < 0.05$; Fig. 1a–f). Together, our findings suggest that Gal-3 potentiates IL-4 and IGF-1 and, to a lesser extent, TGF-β signaling in microglia, suggesting a skewing toward the alternative-activated phenotypes [34].

Previous findings by Lively et al. showed that targeting IL-4 may have an important impact on microglia morphology and motility [35]. IL-4 tyrosine kinase receptors are expressed by microglia, and previous evidence showed that Gal-3 interacts with several tyrosine kinase receptors and growth factor receptors and potentiates their physiological actions [23]. In this context, we next examined whether Gal-3 affects microglia morphology and/or function in an IL-4-dependent manner. We first analyzed the effect of Gal-3 on microglia morphology in vitro (in glutamate-free primary microglia culture). As shown in Fig. 1g–t, immunofluorescence analysis revealed that 24 h following addition of Gal-3 (5 μM), the number and length of filopodia significantly increased in Gal-3-positive cells (***$P < 0.001$; Fig. 1g–n, s, t). Interestingly, administration of CD124, an IL-4 receptor blocker, diminished Gal-3-induced microglia ramification, showing the involvement of IL-4 receptor signaling in Gal-3 effects on microglia morphology (***$P < 0.001$; Fig. 1o–t). As shown in Fig. 1u, v, co-immunoprecipitation experiments revealed the physical interaction between the IL-4 receptor and Gal-3, suggesting that the IL-4 receptor–dependent effects on microglia morphology may, in part, depend on its interaction with Gal-3.

We next investigated functional consequences of the Gal-3-mediated effects on microglia morphology. Previous evidence suggests that an increase in microglia ramifications have an impact on their mobility. In order to determine the effects of Gal-3 on microglial migration, the scratch wound assay was used to analyze migration in 2-D while viewing the cell morphology [32]. Both untreated and Gal-3-treated microglia migrated into the cell-free area, but the mobility of cells receiving Gal-3 at the highest concentration (5 μg/ml) was nearly 2-fold greater (*$P < 0.05$; Fig. 1w). Lower concentrations of Gal-3 (0.1, 1 μg/ml) did not significantly affect microglia migration ($P > 0.05$). Taken together, in in vitro conditions, addition of Gal-3 increases microglia ramification and mobility as well as the levels of some anti-inflammatory cytokines.

Gal-3 Changes Microglia Morphology In Vivo

We next examined effects of Gal-3 on resting microglia cells in vivo in control animals, under physiological conditions. As shown in Fig. 2a, as in in vitro conditions, Gal-3 administration shifted microglial morphology toward a more ramified state 24 h after injection. In fact, intracortical injection of Gal-3 (100 ng/mouse) (Fig. 2e–g) as compared to Mock (Fig. 2b–d), markedly increased the number of visible microglial processes (ramifications) in the injection site (Fig. 2a), resulting in significantly more ramified cells and processes per cell (***$P < 0.001$ and *$P < 0.05$, respectively;

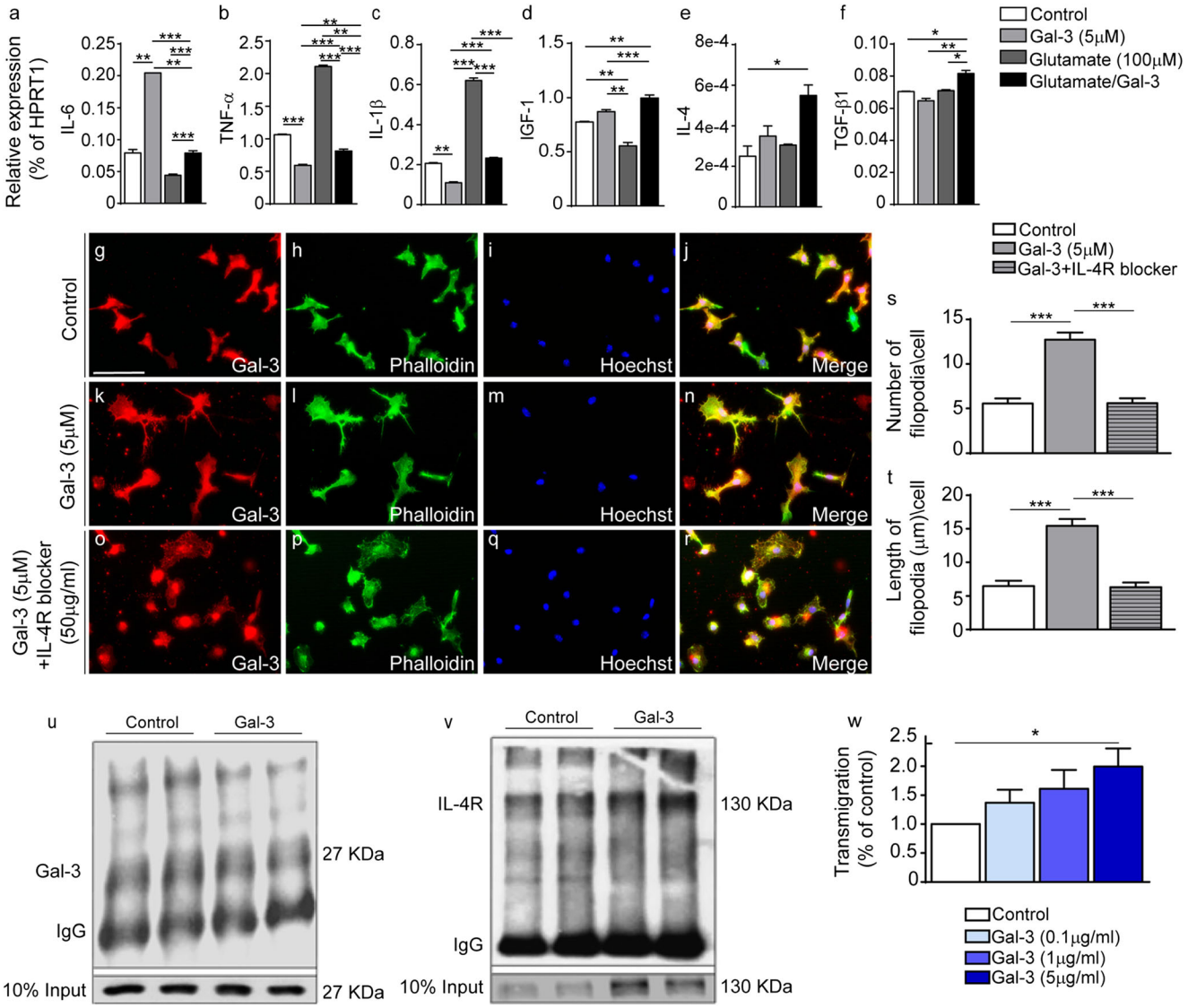

Fig. 1 Gal-3 alters the secretory profile, morphology, and migration pattern of cultured microglia. **a**–**f** Expression analysis of different immunomodulatory molecules in primary microglial cultures by real-time PCR reveals decreased mRNA levels of pro-inflammatory cytokines (TNF-α and IL-1β), increased growth factor levels (TGF-β and IGF-1), and an increase in the anti-inflammatory cytokine IL-4. Values indicate mean ± SEM ($n = 6$, $^{***}P < 0.001$; $^{**}P < 0.01$; $^{*}P < 0.05$). **g**–**t** Primary microglia cell cultures treated with Gal-3 (5 μM) displayed more ramifications. Both the number and the length of filopodia were increased by Gal-3 ($^{***}P < 0.001$). Administration of the IL-4 receptor inhibitor, CD124 (50 μg/ml), completely abolished the effect of Gal-3 on ramification, indicating an IL-4 receptor-dependent action of Gal-3 on morphology. The number (**s**) and length (**t**) of filopodia were quantified. Values indicate mean ± SEM ($n = 6$, $^{***}P < 0.001$; $^{**}P < 0.01$; $^{*}P < 0.05$). **u**, **v** Co-immunoprecipitation experiments using either anti-Gal-3 or anti-IL-4 receptor antibody revealed a physical interaction between the IL-4 receptor and Gal-3. **w** A scratch wound assay has been performed in the presence of different concentrations of Gal-3 (0.1–5 μg/ml). Both untreated (Mock) and Gal-3-treated microglia migrated into the cell-free area 24 h after treatment. Gal-3, at the highest dose (5 μg/ml), significantly increased migration in comparison to control ($P < 0.05$). Values indicate mean ± SEM ($n = 6$, $^{***}P < 0.001$; $^{**}P < 0.01$; $^{*}P < 0.05$)

Fig. 2h, i). Hence, in non-stroked brains, Gal-3 administration has significant impact on microglia morphology.

Gal-3 Induces Alternative Microglial Activation After MCAO

We previously showed that Gal-3 is instrumental in microglial activation responses and TLR2 induction following ischemic injury [13]. Namely Gal-3 deficiency was associated with altered microglial activation and post-stroke inflammation, resulting in larger infarcts. Based on our previous work, here, we examined the potential of using Gal-3 as immunomodulatory molecule. Previously, after MCAO, Gal-3 was strongly induced (peaking between 48 and 72 h) in IGF-positive proliferating resident microglia, which are known to have a protective phenotype [10]. To mimic this "protective temporal dynamics," Gal-3 was now injected i.c.v. in a single dose at 24 h after stroke. As shown in Fig. 3a, to assess the effects of

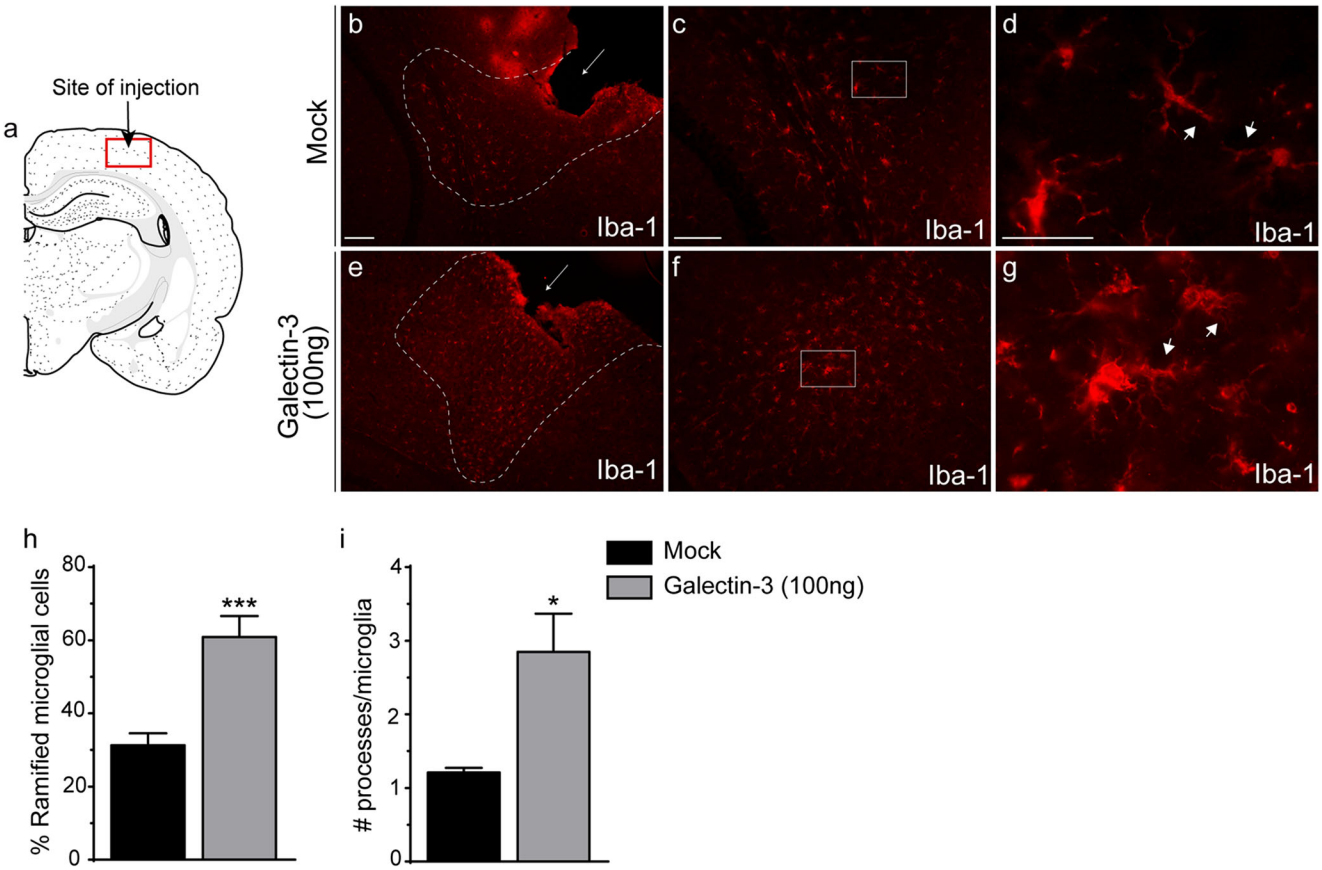

Fig. 2 Gal-3 alters the morphology of microglia in vivo in mice without MCAO. **a**–**g** Immunofluorescence experiments reveal that intracortical Gal-3 administration skews microglia morphology toward a ramified state, as visualized using microglial marker (Iba-1). Gal-3 treatment (**e**–**g**) compared to Mock (**b**–**d**) significantly induced microglial ramification in the vicinity of the injection site, as indicated by increases in both numbers of ramified cells and processes per cell (**h**, **i**). Scale bars represent 500, 100, and 50 μm. Values indicate mean ± SEM ($n = 6$, $^{***}P < 0.001$; $^{**}P < 0.01$; $^{*}P < 0.05$)

Gal-3 after stroke, we took advantage of the TLR2 reporter mouse model and in vivo bioluminescence imaging [24]. The TLR2-driven GFP transgene is strongly induced in microglia in the ipsilateral brain as soon as 24 h after MCAO and can be used as a valid biomarker of microglial activation/innate immune induction after stroke [24, 25]. Quantitative analysis of photon emissions revealed decreased expression of the TLR2 signal 1 day after i.c.v. injection of Gal-3 (48 h post-cerebral ischemia) as compared with the control (Mock-treated) group ($^{*}P < 0.05$; Fig. 3a–g). To further examine the effects of Gal-3 on microglial activation after stroke, we performed double-immunofluorescence analyses of known markers of microglial activation in Gal-3- and Mock-treated mice. The brains were perfused 72 h after stroke (48 h after Gal-3 i.c.v. injection). As shown in Fig. 3h–s, a single dose of Gal-3 recombinant protein 24 h after stroke induced robust microgliosis, characterized by elevated immunoreactivity of Iba1 and Gal-3, as well as Ym1, which is an alternative activation marker engaged in preventing degradation of extracellular matrix components [36]. The immunofluorescence results were further confirmed by Western blot, which revealed upregulation of Iba-1 and Ym1 and downregulation of iNOS expression after Gal-3 injection ($^{**}P < 0.01$; $^{*}P < 0.05$; Fig. 3t–x). Contrary to a robust effect on microglia, delivery of recombinant Gal-3 did not exert significant effects of astrocyte activation and/or morphology, as revealed by GFAP immunostaining and further confirmed by Western blot analysis (Fig. 3y–dd).

A Single Gal-3 Injection Markedly Shifts Cytokine Expression Profiles and Significantly Decreases the Ischemic Lesion

Microglia and macrophages are pivotal for initiation of the inflammatory cascade and can further propagate cell death beyond the initial ischemic region [37, 38]. In contrast, an alternative activation response is needed to properly downregulate inflammation and initiate repair. To further gain insights into the observed Gal-3-mediated shift in the post-stroke microglia activation profiles, we analyzed the impact of a single i.c.v. dose of recombinant Gal-3 on the expression patterns of pro- and anti-inflammatory cytokines. Forty cytokines were analyzed using a multiple

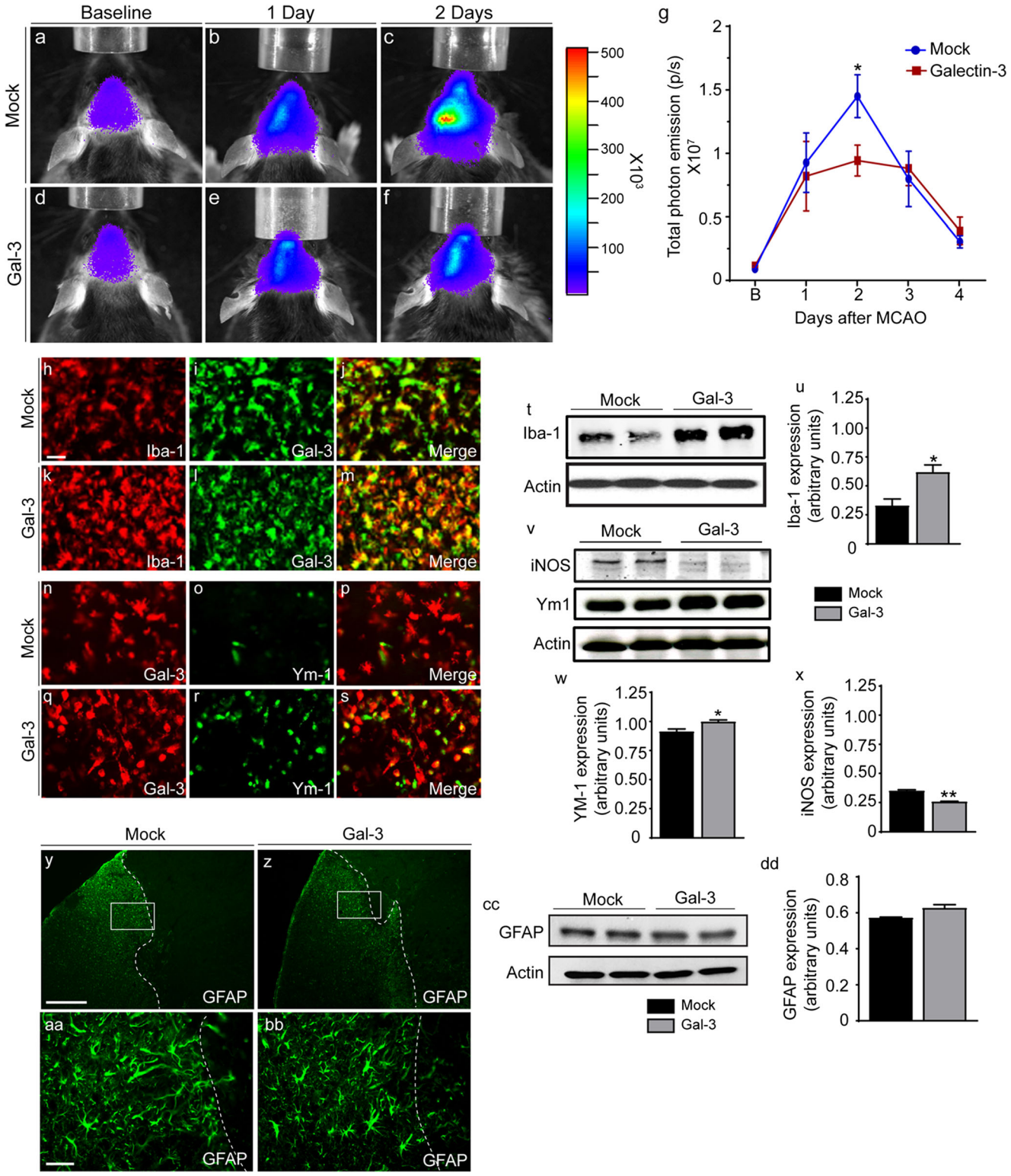

cytokine array system (at 24 h rafter Gal-3 administration; 48 h after stroke). As shown in Fig. 4a–j, a single dose of Gal-3 significantly decreased the level of pro-inflammatory cytokines (TNF-α, IL-1β, IL-6, INF-γ, and IL-17) and significantly increased the level of the anti-inflammatory cytokine, IL-4, as compared to controls (***$P < 0.001$; **$P < 0.01$; *$P < 0.05$; Fig. 4a–j). Consistent with our in vitro findings (see Fig. 1a), Gal-3 treatment induced a small but significant increase in IL-6 (Fig. 4d). Levels of IL-10, IL-13, and the colony-stimulating factors, M-CSF

◀ **Fig. 3** Gal-3 ameliorates the microglia activation/TLR2 response and changes their phenotype after ischemia in vivo. (a–f) Real-time imaging of the TLR2 response following transient MCAO in TLR2-luc-GFP mice revealed lower expression of TLR2 1 day after Gal-3 injection. Images were longitudinally recorded from the same experimental animal revealing the dynamics of the microglial activation/TLR2 response at 1–4 days after MCAO. The scales on the right are the color maps for photon counts. (g) Quantification of luciferase signals using Living Image software (CaliperLS, Alameda, CA, USA). Values indicate mean ± SEM ($n = 12$, $^{*}P < 0.05$). (h–m) Two days after i.c.v. injection of Gal-3 (3 days after MCAO), there were more Gal-3-positive microglial cells (Iba-1^{+}), which is indicative of microglial activation. (n–s) Gal-3 injection increased the number Ym1-positive cells, a marker of microglia alternative activation. (t–x) Western blot analysis confirmed that i.c.v. injection of Gal-3 increased the protein level of Iba-1 and Ym1 and decreased the expression of iNOS ($n = 5$, $^{***}P < 0.001$; $^{**}P < 0.01$; $^{*}P < 0.05$). (y–dd) Two days after i.c.v. injection of Gal-3 (3 days after MCAO), immunofluorescence and Western blot studies revealed that Gal-3 does not have any significant effects of astrocyte morphology and the protein levels of astrocyte marker, GFAP. Scale bars represent 1 mm and 100 μm

and GM-CSF, were not significantly affected by Gal-3 administration (Fig. 4f, h–j). Effects of Gal-3 on other cytokines and chemokines have been provided in Supplementary Fig. 1 and Fig. 2.

To explore whether the Gal-3-induced alterations in cytokine expression levels were associated with neuroprotection, we compared the stroke area in Gal-3-treated mice with the corresponding Mock-treated controls. The stroke area was measured 4 days after stroke, at the end of the in vivo imaging protocol (72 h following Gal-3 administration). As shown in Fig. 4k–m, analysis of the stroke area in cresyl violet-stained brain sections revealed a significant decrease in the size of ischemic lesions in mice receiving Gal-3 i.c.v. ($^{**}P < 0.01$; Fig. 4k–m) when compared to Mock-treated controls. Taken together, our results suggest that the timely delivery of Gal-3 might exert neuroprotection after stroke.

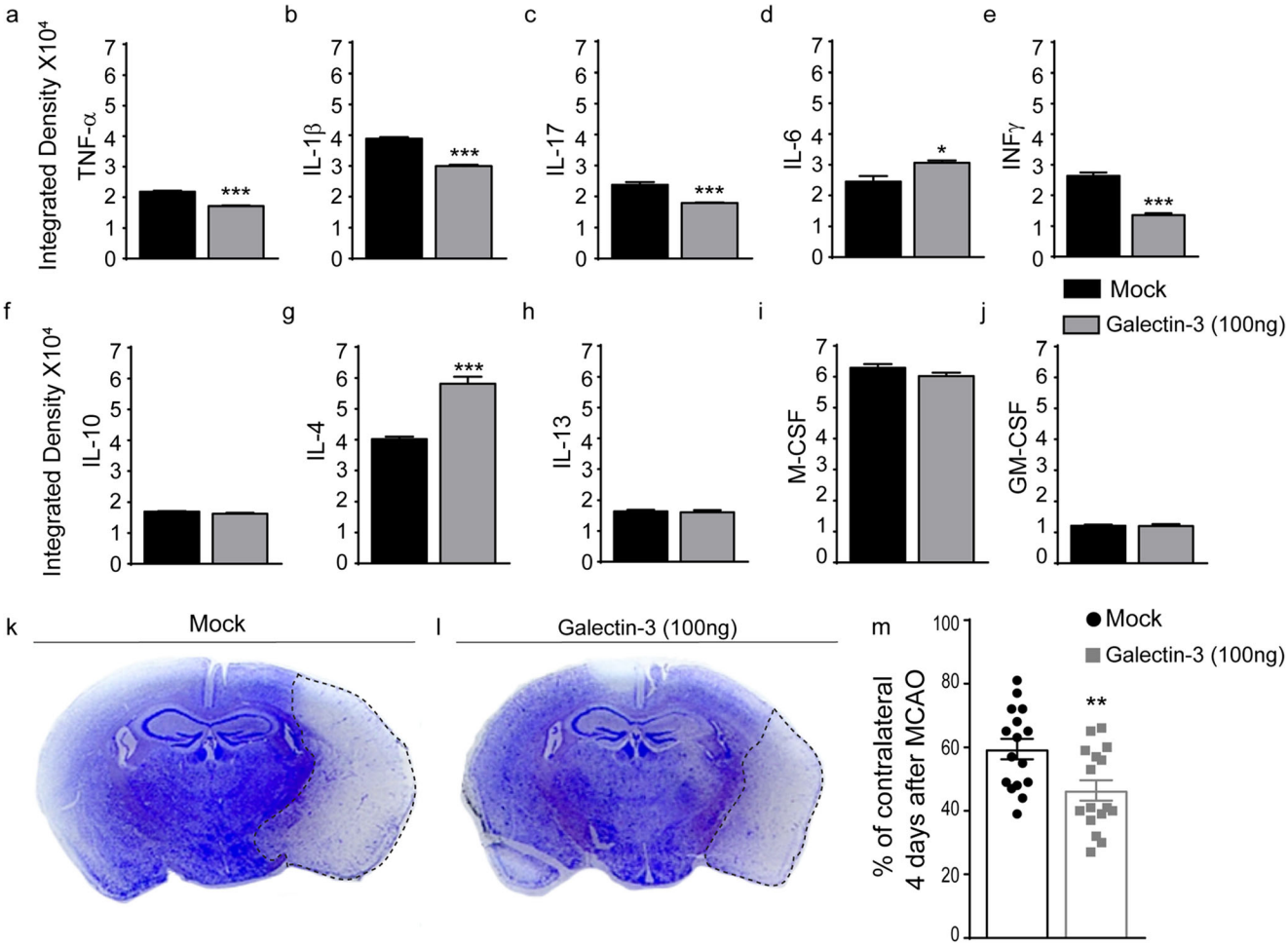

Fig. 4 Gal-3 decreases the expression of pro-inflammatory cytokines and the infarct size after MCAO**. a**–**j** Expression profiles of cytokines after Gal-3 or Mock injection were analyzed. Decreases in the protein levels of pro-inflammatory cytokines (TNF-α, IL-1β, IL-17, INF-γ) (**a**–**c**, **e**) as well as increases in the anti-inflammatory cytokine, IL-4 (**g**), and the pro-inflammatory cytokine, IL-6 (**d**) are observed. Gal-3 administration did not affect the levels of other anti-inflammatory cytokines, including IL-10 and IL-13 (**f**, **h**), or the growth factors, M-CSF and GM-CSF (**i**, **j**). Values indicate mean ± SEM ($n = 3$, $^{***}P < 0.001$; $^{**}P < 0.01$; $^{*}P < 0.05$). **k**–**m** The stroke area was analyzed using cresyl-violet-stained brain sections at day 4 after MCAO. A significant decrease is observed in the size of ischemic lesions in mice receiving i.c.v. Gal-3 injection compared with Mock-treated mice ($P < 0.05$). Values indicate mean ± SEM ($n = 10$, $^{**}P < 0.01$)

Glucosamine Increases Gal-3 Ligand Availability After MCAO and Alters the Morphology and Phenotype of Microglia

In order to further elucidate the molecular mechanisms involved in Gal-3-mediated immunomodulation and neuroprotection, we took advantage of the Gal-3 agonist/modulator, glucosamine. We hypothesized that increasing levels and/or bioavailability of endogenous Gal-3 or its ligands may potentiate Gal-3-mediated neuroprotective effects, such as increases in IL-4 or IGF-1 in microglia. After stroke, glucosamine should increase the intracellular levels of UDP-GLcNA (N-acetylglucosamine) which, in turn, should increase the synthesis and availability of the Gal-3 ligand, and thus increase its binding to the cell surface and promote downstream signaling. To investigate the effects of glucosamine on the synthesis of Gal-3 ligand, biotinylated Gal-3 and a Streptavidin staining system was employed [39]. As shown in Fig. 5a–c, analysis of the brain sections 3 days after MCAO revealed significantly higher levels of ligand (sugar) for Gal-3, compared with control non-treated sections (**$P < 0.01$). The Golgi enzyme, β1,6-N-acetylglucosaminyltransferase V (Mgat5) is the key enzyme in the biosynthesis of N-glycans carrying more than 3 N-acetyllactosamine, the preferred ligand for Gal-3. It has been reported that Gal-3 crosslinks Mgat5-modified N-glycans on epidermal growth factor and other growth factor receptors, at the cell surface and delays their removal by constitutive endocytosis [13, 23]. As shown in Fig. 5d, e, 3 days after MCAO, glucosamine elevated the expression of Mgat5 and consequently increased the availability of Gal-3 ligands, which was confirmed with biotinylated Gal-3 and Streptavidin staining (*$P < 0.05$).

Next, in support of our hypothesis, treatment with glucosamine significantly increased endogenous Gal-3 and IL-4 receptor levels (*$P < 0.05$; Fig. 5f–h). To assess whether glucosamine-mediated increase in endogenous Gal-3 induces a similar shift in microglial activation profiles as observed following recombinant Gal-3 injection, we measured expression levels of microglial markers associated with alternative and classical activation. As shown in Fig. 5i–o, Western blot analysis revealed significant increase in Ym1, Arg1, and IL-4 expression levels while iNOS, CCL5, and TNF-α levels were decreased 3 days after stroke in glucosamine-treated animals (**$P < 0.01$; *$P < 0.05$). Taken together, the results of our study suggest that a timely direct and/or indirect increase in Gal-3 levels shifts microglial activation toward an anti-inflammatory phenotype by promoting IL-4 and IGF-1 signaling [10, 40], and thus exerts neuroprotection.

Glucosamine Increases Microglia Proliferation and IGF-1 Levels Following MCAO

Our previous work described an important role for Gal-3 in IGF-1-mediated microglial proliferation and neuroprotection [13]. As discussed above, the glucosamine-induced Gal-3 upregulation following MCAO increases the availability of Gal-3 ligands and thus may potentiate Gal-3 downstream effects, such as microglia proliferation and growth factor secretion. As shown in Fig. 6a–g, glucosamine increases proliferation of microglial cells as revealed by increased expression levels of Ki-67 (proliferation marker) in Gal-3 expressing microglia (*$P < 0.05$) and significantly increases the overall levels of IGF-1 (**$P < 0.01$; Fig. 6h–n).

Discussion

In the present study, we provide important in vitro and in vivo evidence of the immunomodulatory potential of Gal-3. We showed that Gal-3 modulates the cytokine profile of microglia toward an anti-inflammatory state. In vitro, Gal-3 increases microglial ramification and mobility, the former being elicited in an IL-4 receptor-dependent manner. Importantly, delayed treatment with recombinant Gal-3 after stroke exerted significant neuroprotection. Delivery of Gal-3 24 h after stroke was associated with an increase in Ym1-positive microgliosis and diminished iNOS expression. Analysis of cytokine protein profiles revealed downregulation of pro-inflammatory cytokines and a significant upregulation of the anti-inflammatory cytokine, IL-4. Importantly, the observed shift in microglial activation profiles was associated with a significant decrease in infarct size. Taken together, our results suggest that when delivered late after ischemic injury, Gal-3 acts to fine-tune inflammatory responses by inducing a shift in microglia polarization profiles.

Microglia and macrophages are pivotal for initiating the inflammatory cascade and further propagating cell death beyond the initial ischemic region [37, 38]. In contrast, an alternative activation response is needed to properly downregulate inflammation and initiate repair. Indeed, mice lacking alternative activation signaling molecules, such as IL-4 or IL-10, have worse outcomes after experimental cerebral ischemia [41, 42]. Similarly, Gal-3 deficiency reduces levels of cytokines released by alternative activated microglia, resulting in an aggravated pathology following stroke [13, 22]. This highlights the importance of alternatively activated microglia in mitigating neurotoxic inflammation and repairing damage. In a pioneering study, MacKinnon et al. [43] showed that IL-4-mediated alternative macrophage activation is inhibited by siRNA-driven silencing of Gal-3 or its membrane receptor, CD98, and by inhibition of PI3K. Increased Gal-3 expression and secretion is a feature of alternative macrophage activation. IL-4 stimulates Gal-3 expression and release in parallel with other phenotypic markers of alternative macrophage activation. By contrast, classical macrophage activation with lipopolysaccharide (LPS) inhibits Gal-3 expression and release. IL-4-induced alternative activation is blocked by bis-(3-

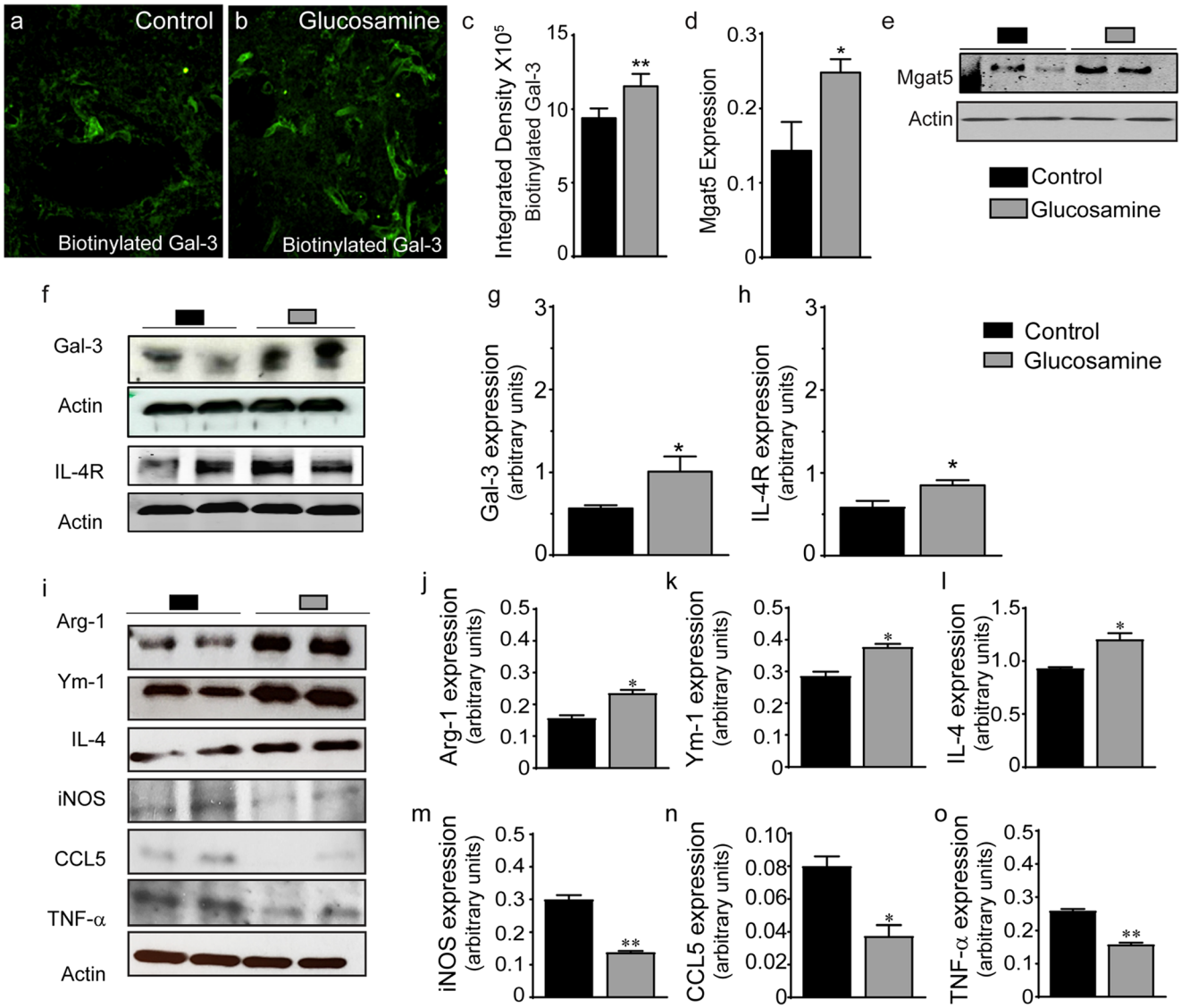

Fig. 5 Glucosamine treatment increases Gal-3 ligand avidity after stroke and induces neuroprotective markers. **a**–**c** Biotinylated Gal-3 and a Streptavidin staining system reveals (in glucosamine-treated sections) higher levels of ligand (sugar) for Gal-3 compared to control nontreated sections. Values indicate mean ± SEM ($n = 6$, $^{*}P < 0.05$). **d**, **e** The Golgi enzyme, Mgat5, promotes the substitution of N-glycan with poly N-acetyllactosamine, the preferred ligand for Gal-3. Three days after MCAO, glucosamine administration increased the expression of Mgat5 significantly and consequently increased the availability of Gal-3 ligands, which confirmed the findings with biotinylated Gal-3 and Streptavidin staining. Values indicate mean ± SEM ($n = 5$, $^{***}P < 0.001$; $^{**}P < 0.01$; $^{*}P < 0.05$). **f**–**h** Glucosamine administration after MCAO induced the expression of Gal-3 and IL-4 receptor in the stroked region ($n = 5$, $^{*}P < 0.05$). **i**–**o** Glucosamine administration following MCAO upregulated the protein levels of Ym1, Arg1, and IL-4 (anti-inflammatory markers) and downregulated the levels of iNOS, CCL5, and TNF-α (pro-inflammatory markers) ($n = 5$, $^{**}P < 0.01$; $^{*}P < 0.05$)

deoxy-3-(3-methoxybenzamido)-β-D-galactopyranosyl) sulfane, a specific inhibitor of extracellular Gal-3 carbohydrate binding. These results demonstrate that a Gal-3 feedback loop drives alternative macrophage activation [43].

Unlike the well-described role of the IL-4/Gal-3 axis in alternative activation of peripheral macrophages described above, its roles in resident microglia remain elusive. The results of our study support the role of Gal-3/IL-4 in modulation of microglia morphology as well as alternative activation. As shown in our in vitro and in vivo experiments, Gal-3 administration induced microglial arborization, as quantified by the length and number of filopodia. Next, administration of an IL-4 receptor blocker reversed the effects of Gal-3 on microglial ramification, while immunoprecipitation studies revealed a physical interaction between the IL-4 receptor and Gal-3 in microglia cell cultures. The capacity of Gal-3 to change the immune profile of microglia/macrophages toward more alternative activated phenotypes was further demonstrated in the MCAO stroke model. A single i.c.v. injection of recombinant Gal-3 delivered 24 h after stroke changed the

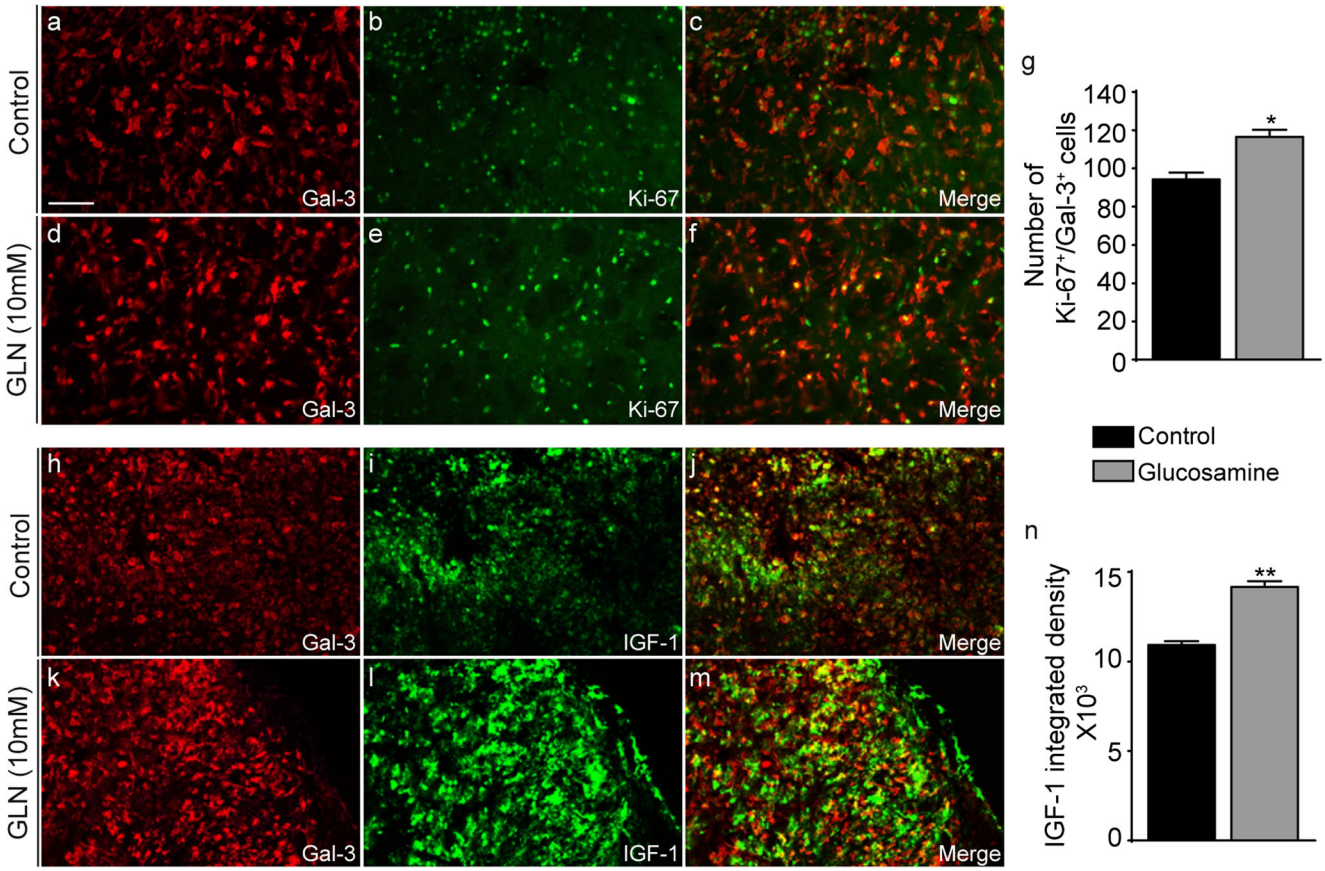

Fig. 6 Glucosamine treatment induces microglia proliferation and upregulates IGF-1 following MCAO. **a**–**g** Three days following MCAO, more proliferating Ki-67-positive cells were detected in glucosamine-treated animals. The majority of Ki67-positive cells co-localized with Gal-3, indicating microglial proliferation ($n = 6$, $^{*}P < 0.05$). **h**–**m** Glucosamine administration increased the overall expression of IGF-1. Furthermore, cytokine array analysis showed that 72 h after MCAO, glucosamine increased the protein level of IGF-1 (**n**). Scale bar represents 100 μm. Values indicate mean ± SEM ($n = 6$, $^{**}P < 0.01$)

cytokine profile toward an anti-inflammatory state. Indeed, this Gal-3 treatment increased expression of Ym1 and diminished iNOS expression 2 days after MCAO. This effect was accompanied by a significant increase in the level of an anti-inflammatory cytokine (IL-4) and a reduction in pro-inflammatory cytokines (TNF-α, IL-1β, IFN-γ, IL-17) in ipsilateral brain regions. Here, it is noteworthy that, in addition to the observed interaction with IL-4, once oligomerized, Gal-3 molecules might crosslink growth factor receptors at the surface and delay their removal by endocytosis, resulting in prolongation of their signaling. Previous work suggests that Gal-3 crosslinks with several growth factor receptors (e.g., IGF-1, EGF) altering downstream signaling [13, 23].

A role for Gal-3 as an endogenous immunomodulatory molecule in the brain remains unclear and controversial. So far, the majority of the Gal-3 functions have been identified in the peripheral immune system [20]. Normally silent, following ischemic injury (within the first 48–72 h), Gal-3 is robustly induced in proliferating microglia, some of which also express growth factor receptors [10, 13]. Of note, ischemic brains of Gal-3KO mice display a 3-fold reduction in proliferating microglia [13]. These findings position Gal-3 as an important mediator of microglial proliferation and activation in brain injury and/or degeneration. Intriguingly, the study by Lalancette-Hébert et al. revealed that Gal-3 deficiency is associated with a marked deregulation of IGF-1-mediated responses to injury, and consequently the inability of microglia to proliferate in response to IGF-1-mediated mitogenic signals [13].

A handful of reports point to multiple functions of Gal-3 in counteracting neuroinflammation. For instance, Gal-3 serves as a receptor for advanced glycation end-products (RAGE) and targets them for lysosomal degradation and removal. As advanced glycation end-products (AGE) are a source of inflammation and oxidative injury in both experimental and clinical amyotrophic lateral sclerosis, deletion of Gal-3 may exacerbate neurodegeneration due to AGE accumulation [44]. Furthermore, Gal-3 was found to be a negative regulator of LPS-induced inflammation; Gal-3 is constitutively produced by macrophages and directly binds to LPS [45]. Gal-3-deficient macrophages have markedly elevated LPS-induced signaling and inflammatory cytokine production compared

with wild-type cells. In the same vein, blocking Gal-3 binding sites using a neutralizing antibody or its lactose-derived chemical antagonist augments LPS-induced inflammatory cytokine expression by wild-type macrophages. In vivo, mice lacking Gal-3 are more susceptible to LPS shock that is associated with excessive induction of inflammatory cytokines and NO production [45]. Hoyos et al. showed that Gal-3 is upregulated in microglia, but not in astrocytes, in response to cuprizone-induced demyelination. This phenomenon favors the remyelination process through induction of alternative activation. Their results highlight Gal-3 as an important modulator of microglia activation and phenotype, the deficiency of which leads to an inability to initiate spontaneous remyelination [46]. Effects of Gal-3 on microglia/macrophage inflammatory signaling are ambiguous, as Gal-3, through interaction with a host of surface receptors and intracellular proteins, can either accentuate or attenuate inflammatory cascades, depending on the context. Apart from the protective role of Gal-3 in post-stroke microglia proliferation in a recent investigation, Burguillos et al. showed that Gal-3 acts as an endogenous TLR4 ligand, thereby initiating a TLR4-dependent inflammatory response in LPS-challenged BV2 microglia [19]. A Gal3-TLR4 detrimental interaction was shown both in a murine model of stroke and in stroke patients [19]. In this context, it has been shown that following head trauma, released Gal-3 may act as an alarmin, binding to TLR-4 and promoting inflammation and neuronal loss [47].

The protective effects of microglia could be mediated by different mechanisms following brain injury [48]. Once activated, microglia can suppress neuroinflammation, restore homeostasis, and protect neurons by producing neurotrophic factors such as neurotrophins and growth factors (IGF-1 and TGF-β). Furthermore, neuroprotective microglia can express markers of antigen-presenting cells, such as MHC-class II and B7.2. These markers interact with lymphocyte with subsequent release of growth factors providing a more suitable environment for neural repair [49, 50]. Microglia might also be beneficial by engulfing neutrophils following ischemic insult and providing neuroprotective phagocytosis [11, 51]. For instance, some studies indicate that phagocytosis of dead cells is crucial to confine secondary damage following brain damage [52]. Finally, some investigations showed that microglia through IGF-1-dependent signaling pathway modulate neurogenesis in subventricular zone after stroke [50, 53].

In summary, in the current study, we used Gal-3 as a molecular tool for elucidating the mechanisms underlying its effect on microglia morphology and phenotype. Microglial activation in ischemic injury is a polarized process. Although therapeutic strategies to shift the balance toward alternative activation are of interest, the regulation of this process in vivo is still largely unknown. Based on our previous work and results of the current study, we propose that when delivered 24 h after stroke, Gal-3 will preferentially interact with microglia growth factor receptors implicated in proliferation and the delayed response to injury; and thus fine-tune and shift the phenotype to more alternative activated, protective phenotypes and exert neuroprotection. However, at this stage, a better understanding of Gal-3 physiology (its extracellular and intracellular effects) and structure (its C-terminal versus N-terminal domains) is instrumental for designing molecules that selectively modulate Gal-3 functions in microglia, skewing them toward an anti-inflammatory phenotype, and therefore could be of more translational value [54].

Funding This work was supported by the Heart and Stroke Foundation of Canada Grant-in Aid no. G-17-0018372 (J.K.)

Compliance with Ethical Standards All experimental procedures were approved (protocol no. 017-133) by the Laval University Animal Care Ethics Committee and are in accordance with the Canadian Council on Animal Care.

Conflict of Interest The authors declare that they have no conflict of interest.

References

1. Prinz M, Priller J (2014) Microglia and brain macrophages in the molecular age: From origin to neuropsychiatric disease. Nat Rev 15(5):300–312. https://doi.org/10.1038/nrn3722
2. Lan X, Han X, Li Q, Yang QW, Wang J (2017) Modulators of microglial activation and polarization after intracerebral haemorrhage. Nat Rev Neurol 13:420–433. https://doi.org/10.1038/nrneurol.2017.69
3. Allan SM, Rothwell NJ (2001) Cytokines and acute neurodegeneration. Nat Rev 2(10):734–744. https://doi.org/10.1038/35094583
4. Iadecola C, Anrather J (2011) The immunology of stroke: from mechanisms to translation. Nat Med 17(7):796–808. https://doi.org/10.1038/nm.2399
5. Benakis C, Garcia-Bonilla L, Iadecola C, Anrather J (2014) The role of microglia and myeloid immune cells in acute cerebral ischemia. Front Cell Neurosci 8:461. https://doi.org/10.3389/fncel.2014.00461
6. Gravel M, Beland LC, Soucy G, Abdelhamid E, Rahimian R, Gravel C, Kriz J (2016) IL-10 controls early microglial phenotypes and disease onset in ALS caused by misfolded superoxide dismutase 1. J Neurosci 36 (3):1031–1048. https://doi.org/10.1523/JNEUROSCI.0854-15.2016, 2016
7. O'Donnell SL, Frederick TJ, Krady JK, Vannucci SJ, Wood TL (2002) IGF-I and microglia/macrophage proliferation in the ischemic mouse brain. Glia 39(1):85–97. https://doi.org/10.1002/glia.10081
8. Nakajima K, Kohsaka S (2004) Microglia: neuroprotective and neurotrophic cells in the central nervous system. Curr Drug Targets Cardiovasc Haematol Disord 4(1):65–84
9. Hanisch UK, Kettenmann H (2007) Microglia: active sensor and versatile effector cells in the normal and pathologic brain. Nat Neurosci 10(11):1387–1394. https://doi.org/10.1038/nn1997
10. Lalancette-Hebert M, Gowing G, Simard A, Weng YC, Kriz J (2007) Selective ablation of proliferating microglial cells exacerbates ischemic injury in the brain. J Neurosci 27(10):2596–2605

11. Neumann J, Sauerzweig S, Ronicke R, Gunzer F, Dinkel K, Ullrich O, Gunzer M, Reymann KG (2008) Microglia cells protect neurons by direct engulfment of invading neutrophil granulocytes: a new mechanism of CNS immune privilege. J Neurosci 28(23):5965–5975. https://doi.org/10.1523/JNEUROSCI.0060-08.2008
12. Bourque JM, Patel CA, Ali MM, Perez M, Watson DD, Beller GA (2013) Prevalence and predictors of ischemia and outcomes in outpatients with diabetes mellitus referred for single-photon emission computed tomography myocardial perfusion imaging. Circ Cardiovasc Imaging 6(3):466–477. https://doi.org/10.1161/CIRCIMAGING.112.000259
13. Lalancette-Hebert M, Swarup V, Beaulieu JM, Bohacek I, Abdelhamid E, Weng YC, Sato S, Kriz J (2012) Galectin-3 is required for resident microglia activation and proliferation in response to ischemic injury. J Neurosci 32(30):10383–10395
14. Sato S, Hughes RC (1994) Regulation of secretion and surface expression of mac-2, a galactoside-binding protein of macrophages. J Biol Chem 269(6):4424–4430
15. Rabinovich GA, Toscano MA, Jackson SS, Vasta GR (2007) Functions of cell surface galectin-glycoprotein lattices. Curr Opin Struct Biol 17(5):513–520. https://doi.org/10.1016/j.sbi.2007.09.002
16. Sato SaR GA (2008) Galectins as danger signals in host-pathogen and host-Tumor interactions:new members of the growng group of alarmins? Galectins. WILEY, Hoboken, New Jersey
17. Sato S, St-Pierre C, Bhaumik P, Nieminen J (2009) Galectins in innate immunity: dual functions of host soluble beta-galactoside-binding lectins as damage-associated molecular patterns (DAMPs) and as receptors for pathogen-associated molecular patterns (PAMPs). Immunol Rev 230(1):172–187. https://doi.org/10.1111/j.1600-065X.2009.00790.x
18. Toscano MA, Ilarregui JM, Bianco GA, Campagna L, Croci DO, Salatino M, Rabinovich GA (2007) Dissecting the pathophysiologic role of endogenous lectins: glycan-binding proteins with cytokine-like activity? Cytokine Growth Factor Rev 18(1–2):57–71. https://doi.org/10.1016/j.cytogfr.2007.01.006
19. Burguillos MA, Svensson M, Schulte T, Boza-Serrano A, Garcia-Quintanilla A, Kavanagh E, Santiago M, Viceconte N et al (2015) Microglia-secreted galectin-3 acts as a toll-like receptor 4 ligand and contributes to microglial activation. Cell Rep 10:1626–1638. https://doi.org/10.1016/j.celrep.2015.02.012
20. Rahimian R, Cordeau P Jr, Kriz J (2018) Brain response to injuries: when microglia go sexist. Neuroscience. https://doi.org/10.1016/j.neuroscience.2018.02.048
21. Ziegler G, Freyer D, Harhausen D, Khojasteh U, Nietfeld W, Trendelenburg G (2011) Blocking TLR2 in vivo protects against accumulation of inflammatory cells and neuronal injury in experimental stroke. J Cereb Blood Flow Metab 31(2):757–766. https://doi.org/10.1038/jcbfm.2010.161
22. Bohacek I, Cordeau P, Lalancette-Hebert M, Gorup D, Weng YC, Gajovic S, Kriz J (2012) Toll-like receptor 2 deficiency leads to delayed exacerbation of ischemic injury. J Neuroinflammation 9:191
23. Partridge EA, Le Roy C, Di Guglielmo GM, Pawling J, Cheung P, Granovsky M, Nabi IR, Wrana JL et al (2004) Regulation of cytokine receptors by Golgi N-glycan processing and endocytosis. Science 306(5693):120–124. https://doi.org/10.1126/science.1102109
24. Lalancette-Hebert M, Phaneuf D, Soucy G, Weng YC, Kriz J (2009) Live imaging of Toll-like receptor 2 response in cerebral ischaemia reveals a role of olfactory bulb microglia as modulators of inflammation. Brain 132(Pt 4):940–954
25. Lalancette-Hebert M, Julien C, Cordeau P, Bohacek I, Weng YC, Calon F, Kriz J (2011) Accumulation of dietary docosahexaenoic acid in the brain attenuates acute immune response and development of postischemic neuronal damage. Stroke 42(10):2903–2909
26. Rancourt A, Dufresne SS, St-Pierre G, Levesque JC, Nakamura H, Kikuchi Y, Satoh MS, Frenette J, Sato S (2018) Galectin-3 and N-acetylglucosamine promote myogenesis and improve skeletal muscle function in the mdx model of Duchenne muscular dystrophy. FASEB journal : official publication of the Federation of American Societies for Experimental Biology:fj201701151RRR. https://doi.org/10.1096/fj.201701151RRR
27. Nieminen J, St-Pierre C, Bhaumik P, Poirier F, Sato S (2008) Role of galectin-3 in leukocyte recruitment in a murine model of lung infection by Streptococcus pneumoniae. J Immunol 180(4):2466–2473
28. Pelletier I, Sato S (2002) Specific recognition and cleavage of galectin-3 by Leishmania major through species-specific polygalactose epitope. J Biol Chem 277(20):17663–17670. https://doi.org/10.1074/jbc.M201562200
29. St-Pierre C, Ouellet M, Tremblay MJ, Sato S (2010) Galectin-1 and HIV-1 infection. Methods Enzymol 480:267–294. https://doi.org/10.1016/S0076-6879(10)80013-8
30. Cordeau P, Kriz J (2012) Real-time imaging after cerebral ischemia: model systems for visualization of inflammation and neuronal repair. Methods Enzymol 506:117–133
31. Cordeau P Jr, Lalancette-Hebert M, Weng YC, Kriz J (2008) Live imaging of neuroinflammation reveals sex and estrogen effects on astrocyte response to ischemic injury. Stroke 39(3):935–942
32. Lively S, Schlichter LC (2013) The microglial activation state regulates migration and roles of matrix-dissolving enzymes for invasion. J Neuroinflammation 10:75. https://doi.org/10.1186/1742-2094-10-75
33. Rahimian R, Dehpour AR, Fakhfouri G, Khorramizadeh MR, Ghia JE, Seyedabadi M, Caldarelli A, Mousavizadeh K et al (2011) Tropisetron upregulates cannabinoid CB1 receptors in cerebellar granule cells: possible involvement of calcineurin. Brain Res 1417:1–8. https://doi.org/10.1016/j.brainres.2011.08.050
34. Butovsky O, Jedrychowski MP, Moore CS, Cialic R, Lanser AJ, Gabriely G, Koeglsperger T, Dake B et al (2014) Identification of a unique TGF-beta-dependent molecular and functional signature in microglia. Nat Neurosci 17(1):131–143. https://doi.org/10.1038/nn.3599
35. Lively S, Hutchings S, Schlichter LC (2016) Molecular and cellular responses to interleukin-4 treatment in a rat model of transient ischemia. J Neuropathol Exp Neurol 75:1058–1071. https://doi.org/10.1093/jnen/nlw081
36. Cherry JD, Olschowka JA, O'Banion MK (2014) Neuroinflammation and M2 microglia: the good, the bad, and the inflamed. J Neuroinflammation 11:98. https://doi.org/10.1186/1742-2094-11-98
37. Schilling M, Besselmann M, Muller M, Strecker JK, Ringelstein EB, Kiefer R (2005) Predominant phagocytic activity of resident microglia over hematogenous macrophages following transient focal cerebral ischemia: an investigation using green fluorescent protein transgenic bone marrow chimeric mice. Exp Neurol 196(2):290–297. https://doi.org/10.1016/j.expneurol.2005.08.004
38. Denker SP, Ji S, Dingman A, Lee SY, Derugin N, Wendland MF, Vexler ZS (2007) Macrophages are comprised of resident brain microglia not infiltrating peripheral monocytes acutely after neonatal stroke. J Neurochem 100(4):893–904. https://doi.org/10.1111/j.1471-4159.2006.04162.x
39. Bhaumik P, St-Pierre G, Milot V, St-Pierre C, Sato S (2013) Galectin-3 facilitates neutrophil recruitment as an innate immune response to a parasitic protozoa cutaneous infection. J Immunol 190(2):630–640. https://doi.org/10.4049/jimmunol.1103197
40. Butovsky O, Ziv Y, Schwartz A, Landa G, Talpalar AE, Pluchino S, Martino G, Schwartz M (2006) Microglia activated by IL-4 or IFN-gamma differentially induce neurogenesis and oligodendrogenesis from adult stem/progenitor cells. Mol Cell Neurosci 31(1):149–160. https://doi.org/10.1016/j.mcn.2005.10.006
41. Xiong X, Barreto GE, Xu L, Ouyang YB, Xie X, Giffard RG (2011) Increased brain injury and worsened neurological outcome in interleukin-4 knockout mice after transient focal cerebral ischemia. Stroke 42(7):2026–2032. https://doi.org/10.1161/STROKEAHA.110.593772

42. Perez-de Puig I, Miro F, Salas-Perdomo A, Bonfill-Teixidor E, Ferrer-Ferrer M, Marquez-Kisinousky L, Planas AM (2013) IL-10 deficiency exacerbates the brain inflammatory response to permanent ischemia without preventing resolution of the lesion. J Cereb Blood Flow Metab 33(12):1955–1966. https://doi.org/10.1038/jcbfm.2013.155
43. MacKinnon AC, Farnworth SL, Hodkinson PS, Henderson NC, Atkinson KM, Leffler H, Nilsson UJ, Haslett C et al (2008) Regulation of alternative macrophage activation by galectin-3. J Immunol 180(4):2650–2658
44. Lerman BJ, Hoffman EP, Sutherland ML, Bouri K, Hsu DK, Liu FT, Rothstein JD, Knoblach SM (2012) Deletion of galectin-3 exacerbates microglial activation and accelerates disease progression and demise in a SOD1(G93A) mouse model of amyotrophic lateral sclerosis. Brain Behav 2(5):563–575. https://doi.org/10.1002/brb3.75
45. Li Y, Komai-Koma M, Gilchrist DS, Hsu DK, Liu FT, Springall T, Xu D (2008) Galectin-3 is a negative regulator of lipopolysaccharide-mediated inflammation. J Immunol 181(4):2781–2789
46. Hoyos HC, Rinaldi M, Mendez-Huergo SP, Marder M, Rabinovich GA, Pasquini JM, Pasquini LA (2014) Galectin-3 controls the response of microglial cells to limit cuprizone-induced demyelination. Neurobiol Dis 62:441–455. https://doi.org/10.1016/j.nbd.2013.10.023
47. Yip PK, Carrillo-Jimenez A, King P, Vilalta A, Nomura K, Chau CC, Egerton AM, Liu ZH et al (2017) Galectin-3 released in response to traumatic brain injury acts as an alarmin orchestrating brain immune response and promoting neurodegeneration. Sci Rep 7:41689. https://doi.org/10.1038/srep41689
48. Schwartz M, Butovsky O, Bruck W, Hanisch UK (2006) Microglial phenotype: is the commitment reversible? Trends Neurosci 29(2):68–74. https://doi.org/10.1016/j.tins.2005.12.005
49. Butovsky O, Hauben E, Schwartz M (2001) Morphological aspects of spinal cord autoimmune neuroprotection: colocalization of T cells with B7–2 (CD86) and prevention of cyst formation. FASEB J : Off Publ Fed Am Soc Exp Biol 15(6):1065–1067
50. Gomes-Leal W (2012) Microglial physiopathology: how to explain the dual role of microglia after acute neural disorders? Brain Behav 2(3):345–356. https://doi.org/10.1002/brb3.51
51. Neumann M, Sampathu DM, Kwong LK, Truax AC, Micsenyi MC, Chou TT, Bruce J, Schuck T et al (2006) Ubiquitinated TDP-43 in frontotemporal lobar degeneration and amyotrophic lateral sclerosis. Science 314(5796):130–133. https://doi.org/10.1126/science.1134108
52. Zhao X, Sun G, Zhang J, Strong R, Song W, Gonzales N, Grotta JC, Aronowski J (2007) Hematoma resolution as a target for intracerebral hemorrhage treatment: role for peroxisome proliferator-activated receptor gamma in microglia/macrophages. Ann Neurol 61(4):352–362. https://doi.org/10.1002/ana.21097
53. Thored P, Heldmann U, Gomes-Leal W, Gisler R, Darsalia V, Taneera J, Nygren JM, Jacobsen SE et al (2009) Long-term accumulation of microglia with proneurogenic phenotype concomitant with persistent neurogenesis in adult subventricular zone after stroke. Glia 57(8):835–849. https://doi.org/10.1002/glia.20810
54. Rahimian R, Beland LC, Kriz J (2017) Galectin-3: mediator of microglia responses in injured brain. Drug Discov Today 23:375–381. https://doi.org/10.1016/j.drudis.2017.11.004